



## OPEN

# Symmetrically periodic segregation in a vertically vibrated binary granular bed

SUBJECT AREAS:

SOFT MATERIALS

NONLINEAR PHENOMENA

Pingping Wen<sup>1</sup>, Ning Zheng<sup>1,2</sup>, Liangsheng Li<sup>3</sup> & Qingfan Shi<sup>1</sup><sup>1</sup>School of Physics, Beijing Institute of Technology, Beijing 100081, China, <sup>2</sup>Key Laboratory of Cluster Science of Ministry of Education, Beijing 100081, China, <sup>3</sup>Science and Technology on Electromagnetic Scattering Laboratory, Beijing 100854, China.Received  
2 July 2014Accepted  
15 October 2014Published  
5 November 2014Correspondence and  
requests for materials  
should be addressed to  
N.Z. (ningzheng@bit.  
edu.cn)

Periodic segregation behaviors in fine mixtures of copper and alumina particles, including both percolation and eruption stages, are experimentally investigated by varying the ambient air pressure and vibrational acceleration. For the cases with moderate air pressure, the heaping profile of the granular bed keeps symmetrical in the whole periodic segregation. The symmetrical shape of the upper surface of the granular bed in the eruption stage, which resembles a miniature volcanic eruption, could be described by the Mogi model that illuminates the genuine volcanic eruption in the geography. When the air pressure increases, an asymmetrical heaping profile is observed in the eruption stage of periodic segregation. With using the image processing technique, we estimate a relative height difference between the copper and the alumina particles as the order parameter to quantitatively characterize the evolution of periodic segregation. Both eruption and percolation time, extracted from the order parameter, are plotted as a function of the vibration strength. Finally, we briefly discuss the air effect on the granular segregation behaviors.

Granular segregation induced by external excitation is of importance in industrial and scientific society, widely applied in the agriculture, food and pharmaceutical processing, and ore dressing<sup>1–4</sup>. In last two decades, shaken, sliding or rotary segregation of binary particles exhibits various patterns, such as the well-known Brazil nut effect (BNE)<sup>3,4</sup>, reverse Brazil nut effect (RBNE)<sup>5,6</sup>, sandwich pattern (SP)<sup>7</sup>, axial or radial streaks<sup>8–10</sup>, and sliding spontaneous stratification<sup>11,12</sup> etc. Different mechanisms including void filling (also called percolation, small particles tend to fall downward through the gaps in between the large particles)<sup>5,13,14</sup>, density-driven<sup>6</sup>, inertia<sup>7</sup>, buoyancy<sup>15</sup>, convection<sup>16</sup>, geometric shape of particles<sup>17</sup>, the influence of different frictions<sup>18</sup> and interstitial media<sup>19</sup>, were presented to account for these seemingly simple segregation behaviors. Afterwards it is found that in many situations one or several of these mechanisms simultaneously take effect on the segregation, each being dominant in different parameter regimes and thus leading to this complexity<sup>20,21</sup>. However, most experiments and theories only concentrate on the time-independent segregation, in which once spatial pattern is formed, the configuration of the whole granular bed remains a steady state.

Compared with segregation with stable spatial patterns, few well-segregated configurations are time-dependent. Burtally et al observed that the upper surface and the separation boundary periodically swing together back and forth between two alternative configurations where both surfaces were tilted at an angle close to the dynamical repose angle<sup>22</sup>. Strictly speaking, the boundaries were time-dependent, but the basic configurations of the granular bed at all times were unchanged. Until recently, we have observed that in some regimes of specific shaken parameters, the configuration of a copper and alumina mixture evolves with time development, showing the time-dependence characteristic<sup>23</sup>. Traditionally, segregation experiments are performed at atmospheric pressure. However, researches have demonstrated that interstitial air plays an important role on segregation of granular materials<sup>24–26</sup>, which suggests that the manipulation of the air pressure may introduce a wealth of new time-dependent segregation phenomena, providing more information for the deep understanding of the time-dependent separation behaviors.

In this study, we observe a time-dependent periodic segregation (PS) behavior in a vertically vibrated binary granular mixture. When tuning the pressure of interstitial air, the PS exhibits two different forms: symmetrically periodic segregation (SPS) at the region of low air pressure and asymmetrically periodic segregation (APS) at the region of high air pressure. Here we systematically investigate the SPS behavior. We first use a sequence of successive snapshots to illustrate two alternating stages in the SPS pattern: the percolation stage where the alumina particles pass through the copper layer and assemble at the bottom; the eruption stage where the deposited alumina layer heaps and then surges onto the top from the middle of the upper copper layer, which looks like a miniature volcanic eruption. To quantitatively characterize the periodic behaviors, we introduce an order parameter defined as a relative height difference between copper and alumina particles by the image processing



technique. Not only can the order parameter be used to extract the percolation time, eruption time and whole period of the SPS quantitatively and accurately, but to characterize every status in time-dependent segregation. With the aid of the order parameter, we plot the periodic time at the percolation and the eruption stage as a function of vibrational acceleration  $\Gamma$ . We also concern about the eruption stage in SPS since it appears analogous to a volcanic eruption in nature. Thus we attempt to apply Mogi model which was a classical model in the earthquake field for the deformational evolution of the earth surface<sup>27</sup>, to fit the arching profile of upper surface of the granular bed. It is surprisingly found that the model is able to describe the deformational evolution of the upper surface of the granular volcano. Finally, we briefly discuss the APS pattern and the air effect on the granular segregation.

## Results

**Experimental setup.** A vertical vibration system is used to investigate the periodic segregation behaviors of the fine mixture. The fundamental diagram of the experimental establishment is illustrated in Fig. 1. A top-opened rectangular glass container with a size 40 mm (length)  $\times$  10 mm (width)  $\times$  50 mm (height) is mounted on the platform of an electromechanical shaker that is used to generate vertical sinusoidal motion, with the ratio of the horizontal vibration amplitude to the vertical vibration amplitude less than 3%. An accelerometer continuously monitors the vertical vibration, which is conveniently characterized by two control parameters  $f$  and  $\Gamma = 4A\pi^2f^2/g$ , where  $f$  is the vibrational frequency, and  $\Gamma$  is a dimensionless acceleration, namely the ratio of the maximum acceleration of the shaker to the gravitational acceleration  $g$ ,  $A$  is the vibration amplitude. In this experiment, we choose the frequency  $f$  at 42 Hz and the acceleration  $\Gamma$  within the ranges of 5.4–6.8. A plexiglass cylinder, of a diameter 120 mm and a height 240 mm, bolted to the shaker acts as a vacuum chamber which

can be evacuated to a lowest pressure around 30 Pa through a mechanical pump. By rotating a fine tuning valve on the chamber, the background air pressure inside the chamber can be quantitatively adjusted.

The binary mixture in the glass container consists of copper particles of density 8.38 g/cm<sup>3</sup> and of diameter  $320 \pm 30 \mu\text{m}$  and alumina particles of density 1.65 g/cm<sup>3</sup> and of diameter  $170 \pm 10 \mu\text{m}$ . Unless specified otherwise, each volume of the granular components, in the proportion 50% : 50%, used in the binary mixture is 3 ml for all experimental trials. Before the experiment, both types of particles are mixed intimately and handled by an antielectrostatic process. To eliminate the build-up of static charges, we replace the mixture by freshly prepared particles every 20 min, and maintain the humidity of the laboratory at the range of 45%–55%. After all experimental conditions are well established, we use a digital camcorder to record the spatial configuration of the granular bed, and also apply a high-speed camera (Phantom V7.3) to capture the details of the dynamical deformation process of the upper surface of the granular bed.

**Phase diagram.** Vibrating patterns of the binary mixture at various air pressures and dimensionless accelerations are recorded. To avoid the air flow caused by the pump evacuation, the mechanical pump is halted before turning on the shaker. The initial status of the mixture is always mixed state, and all stable configurations are identified as a pattern that may be maintained at least ten min at given conditions.

Fig. 2 represents the regions of different patterns in the  $\Gamma$ - $P$  plane. At low pressure region, the mixture retains a mixed state (MS) and no segregation behaviors are observed. Any tendency to separate particles is thwarted by strong global convection. As the air pressure is steadily increased, a segregation behavior emerges. The mixture first evolves into a spatial configuration of one single copper rich layer sandwiched between two alumina rich layers in seconds. Subsequently, the alumina particles on the top percolate through

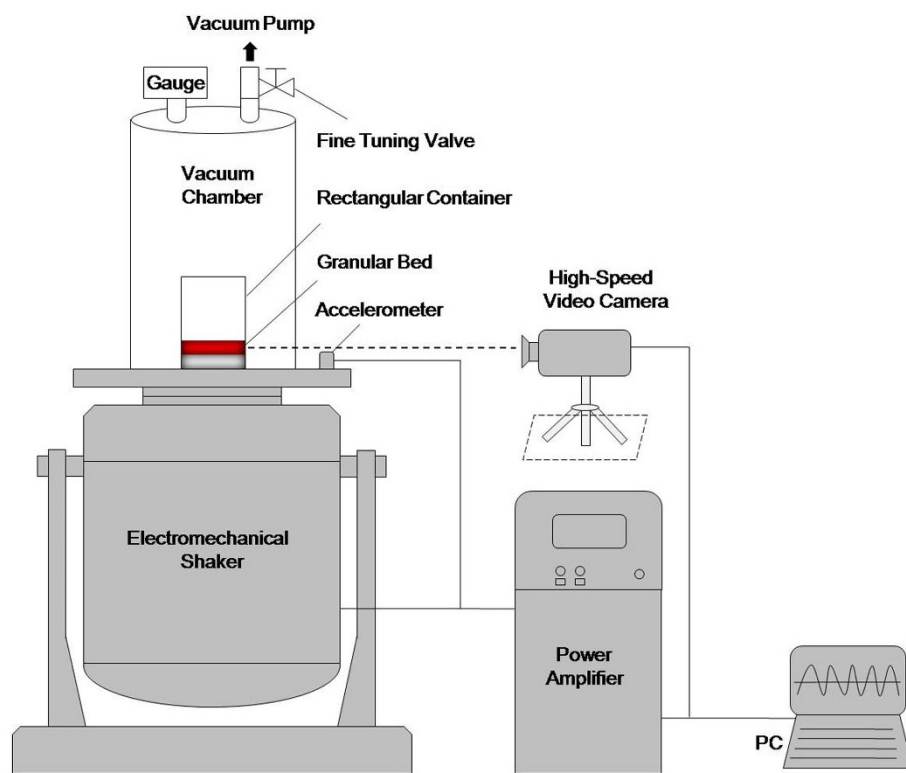


**Figure 1** | Schematic diagram of the experimental apparatus is shown. The vibrational system is fully automated and controlled by a computer. A vacuum gauge measures the background air pressure inside the cylindrical chamber. A high-resolution digital camcorder a high-speed camera sits in front of the container, recording the spatial configuration of the binary granular bed in the view of the large face (40 mm  $\times$  50 mm) of the container.

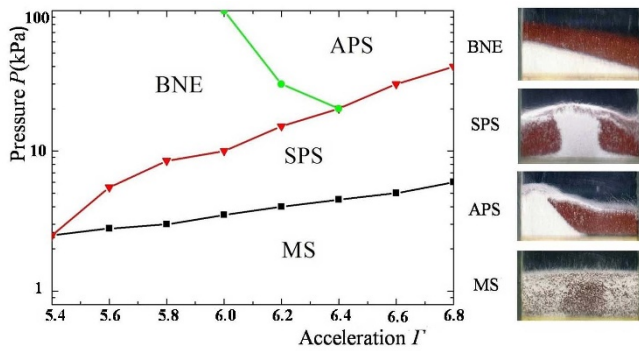


**Figure 2** | Schematic air pressure  $P$  Vs dimensionless acceleration  $\Gamma$  phase diagram for a binary mixture of copper-alumina particles. The copper particles are dark red, and the alumina particles are white. Solid lines are drawn to guide the eye. Region MS: mixed state; BNE: Brazil nut effect segregation; SPS: symmetrically periodic segregation; APS: asymmetrically periodic segregation. Typical configurations shown by these photographs on the right: BNE segregation, symmetrically periodic segregation, asymmetrically periodic segregation and mixed state.

the copper layer and accumulate on the bottom, and thus the two alumina layers merge into one. The final configuration which large particles move to the top of a collection of small particles is the well-known BNE. The boundary of the two components is not necessarily horizontal for BNE; two types of heaping boundaries are observed. When the air pressure is relatively low, a symmetrical heap occasionally occurs in the middle of the container. Remarkably, the symmetrical heap is unstable and soon vanishes, and then reappears after a while, forming an oscillation. At the region with high air pressure and large value of  $\Gamma$ , an asymmetrical heap always arises and it is a stable configuration (see the inset in Fig. 2). Whatever the boundary looks like, the spatial configuration of BNE is time-independent. When  $\Gamma$  continues to increase, the mixture enters into a time-dependent segregation status, namely the PS region. In this region, either the symmetrical or the asymmetrical heap keeps growing until the heap breaks through the suppression of the upper copper layer, surging onto the top surface. According to the difference from the spatial conformation of the eruption stage, we divide the PS into two categories, the symmetrical PS pattern (SPS) and the asymmetrical PS pattern (APS). The corresponding insets in Fig. 2 illustrate the inversion moments of alumina particles for two patterns. The APS takes place in the high pressure regime. In contrast, the SPS is a new type of periodic segregation which always occurs at low air pressure, as shown in Fig. 2. Next we focus on the SPS pattern as a detailed investigation of the PS behaviors.

**Symmetrically periodic segregation.** Fig. 3 illustrates a complete cycle of the segregation using a series of consecutive snapshots at  $P = 7$  kPa and  $\Gamma = 6.4$ . Initially the mixture is vibrated for a while, forming a RBNE configuration, as shown in Fig. 3(a). However, the RBNE is unstable. As more time elapses, the alumina particles percolate through the copper layer and constitute a new layer below the copper one; the RBNE evolves to be a sandwich pattern [Fig. 3(b)]. With the amount of alumina particles on the top layer steadily decreasing, the alumina particles finally deposit at the bottom of the container, developing into a BNE configuration [see Fig. 3(c)]. Here it is natural that the duration from Fig. 3(a) to Fig. 3(c) is defined as the percolation stage. It should be pointed out that BNE is not final state for the system. The horizontal alumina layer becomes unstable; namely the alumina particles begin to gather in the middle of the granular bed, forming a symmetrical heap, as shown in Fig. 3(d). The symmetrical alumina heap gradually grows and eventually breaks through the upper copper layer, surging onto the top. The duration from Fig. 3(c) to

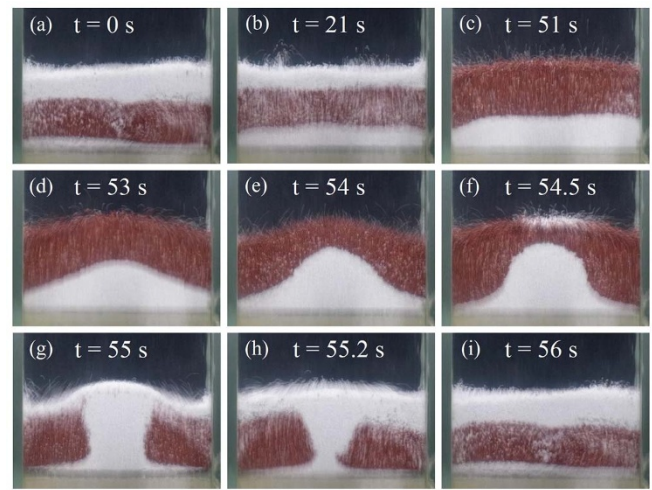


**Figure 3** | Series of consecutive snapshots, extracted from a video which records a typical symmetrical periodic segregation at  $p = 7$  kPa and  $\Gamma = 6.4$ , represent a complete cycle with a time scale. Here the dark particles are copper and the white particles are alumina. The percolation stage: (a) – (c); the eruption stage: (c) – (i).

Fig. 3(i) is referred to as the eruption stage; including the heaping process or called the pre-eruption process [see Fig. 3(c)–Fig. 3(f)] and the inversion process [refer to Fig. 3(f)–Fig. 3(i)], which resembles a miniature volcano being in violent eruption. In general, the granular bed in SPS undergoes a stable cycle of RBNE-SP-BNE-RBNE, which consists of the percolation and the eruption stage.

**Relative height difference  $\phi$ .** To date, the segregation behaviors in most literatures were described with qualitative methods, for instance, BNE or RBNE pattern was judged only by the photo images. The approach for quantitatively determining the segregation degree is still scarce. Even if a quantitative definition was presented to differentiate the pure segregation from light mixed state, the requirement of a flat boundary of the separated layers restricted its application<sup>6</sup>. Particularly, if the segregation behavior is time-dependent, such an approach in Ref. 6 for various segregation patterns becomes inaccurate and inconvenient. In order to quantitatively characterize the time-dependent segregation patterns, we introduce a relative height difference  $\phi$  between copper and alumina particles by using the image processing technique

$$\phi = \frac{\sum_{i=1}^{N_{Cu}} p_i^{Cu}/N_{Cu} - \sum_{i=1}^{N_{Al}} p_i^{Al}/N_{Al}}{\sum_{i=1}^{N_{Cu}} p_i^{Cu}/N_{Cu} + \sum_{i=1}^{N_{Al}} p_i^{Al}/N_{Al}}, \quad (1)$$

Where  $p_i^{Cu}$  and  $p_i^{Al}$  are height coordinates of pixels of copper and alumina particles, and  $N_{Cu}$  and  $N_{Al}$  are the numbers of pixels of copper and alumina particles in a snapshot. The container is reasonably considered quasi-two dimension<sup>30</sup>, and we have observed almost identical configuration of the granular bed at the opposite large face of the container. In this sense, the relative height difference  $\phi$  can be applied to estimate the normalized relative position of the centroids of two components in the granular bed. We can utilize this relative height difference  $\phi$  as an order parameter to distinguish different segregation states. Fig. 4 shows a time evolution of the order parameter in five SPS periods at  $P = 7$  kPa and  $\Gamma = 6.4$ . The excellent repeatability of the order parameter indicates the periodicity of the SPS behavior. Furthermore, the





time at the percolation and the eruption stage can be extracted from Fig. 4. Combining with the visual observation, we build the corresponding relations between the order parameter and the real physical process, see Fig. 4. The order parameter  $\phi$  at point *a* gains a maximum negative value, which means two species of particles have reached a high degree of separation. The centroid of the copper particles is lower than that of the alumina particles, and the case implies a RBNE status [see Fig. 3(a)]. Similarly, the maximum positive value of the order parameter  $\phi$  at point *c* corresponds to a BNE state. The duration from the RBNE to the BNE, namely from  $\phi(a)$  to  $\phi(c)$  is the percolation stage. The sharp decrease of the order parameter from point *c* to point *i* suggests a dramatic transformation of the spatial configuration of the granular bed, and corresponds to the eruption stage. The corresponding relation demonstrates that the relative height difference  $\phi$  can precisely distinguish different segregation states in the time-dependent segregation behavior, and quantitatively and conveniently extract the percolation and the eruption time, which are used to investigate the relations with the external driving parameters, see Fig. 5.

**Periodic time.** In this section, we measure the percolation time  $T_p$ , the eruption time  $T_e$ , and whole cycle time  $T_c = T_p + T_e$  as a function of the vibration acceleration  $\Gamma$  in SPS, respectively. The measurements apparently show a non-monotonic dependence of the percolation time on the vibration acceleration, whereas the eruption time exhibits a monotonic relation. The monotonic decrease of the eruption time indicates that it is easier for the alumina layer to break the suppression of the copper layer with stronger vibrations. At a higher  $\Gamma$ , once most alumina particles have accumulated below the copper layer, the symmetrical heap immediately grows. While at a lower  $\Gamma$ , the heap of the alumina layer does not start until the copper layer becomes more pure. It is worth noting that for all  $\Gamma$ , it only takes several seconds from the onset of the heap to the end of the eruption.

Furthermore, when  $\Gamma > 6.2$ , the eruption time approaches a stable value which is small compared with the percolation time. Thus, the whole cycle time is dominated by the percolation time, basically following the curve shape of percolation time except  $\Gamma < 6.2$ . The non-monotonic behavior implies that underlying physics still keeps open.

**Mogi model.** In a mono-disperse granular system, the center-heaping formations derive from the instabilities of the flat surface,

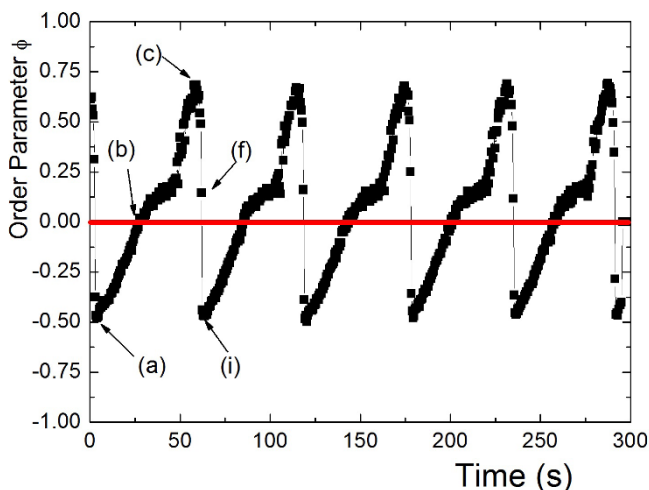


**Figure 4** | Relative height difference  $\phi$ , as an order parameter describes the periodicity and segregation states of the SPS pattern at  $p = 7$  kPa and  $\Gamma = 6.4$ . With using the same letters in Fig. 3, (a) – (c) corresponds to the percolation stage, and (c) – (i) corresponds to the eruption stage. The order parameter can determine the percolation and the eruption time precisely and conveniently.

and the underlying mechanism attributes to downward convection<sup>28,29</sup>. However, for a bi-disperse granular bed, the deformation of the arched profile of upper surface in eruption stage more likely originates from the heaping push of the bottom layer. It can be clearly seen that the arch of the upper surface is much gentler than that of the interface between the two layers [see fig. 3(e)]. Thus single-layer heaping model may not be applicable for this bottom-heap-pushed deformation of the upper surface. Visually, the symmetrical eruption stage is similar to the process of a volcanic eruption in nature, and hence we attempt to introduce the Mogi model<sup>27</sup> to fit the profile of the upper surface. To obtain the profile evolution throughout the eruption stage, we use a high-speed camera at a sample rate 400 fps. We average the 400 pictures to acquire the topography of the upper surface in one second, and to eliminate the profile fluctuation of the upper surface. The topography of the upper surface is averaged as

$$H(x,t) = \frac{1}{N} \sum_{i=1}^N h_i(x,t) \quad (2)$$

Here  $x$  is the horizontal coordinate of the upper surface and  $H(x,t)$  is the height of the surface from the bottom of the container [see the illustration in Fig. 6(a)]. We then apply the Mogi model to fit the averaged profile as follows<sup>27</sup>,

$$\Delta H(x,t) = H(x,t) - H_0 = \frac{Vd}{((x-x_0)^2 + d^2)^{3/2}} \quad (3)$$

Where  $H_0$  is the height of the granular bed at rest,  $x_0$  is the horizontal projection of the upper surface center,  $V$  and  $d$  are fitting parameters. When  $x = x_0$ ,  $H(x,t)$  is the apex of the profile. Then,

$$\Delta H_{\max}(x_0,t) = H(x_0,t) - H_0 = \frac{V}{d^2} \quad (4)$$

Therefore, the upper surface profile can be fitted by the equation below,

$$\Delta H(x,t) = \frac{V^{3/2}}{\sqrt{\Delta H_{\max}}((x-x_0)^2 + V/\Delta H_{\max})^{3/2}} \quad (5)$$

In our experiment,  $H_0$ ,  $\Delta H_{\max}$  and  $x_0$  are measurable parameters, and thus  $V$  is the only fitting parameter. Fig. 6(b) shows the comparison between the fitting result from Eq. (5) and the averaged experimental profile in four seconds at  $f = 42$  Hz,  $\Gamma = 6.2$  and  $P = 7$  kPa. The result shows that the Mogi curves are in good agreement with the topographic growth of the upper surface. Fig. 6(I)–(IV) illustrate the profile evolution of the upper surface with four consecutive figures in a more intuitive way.

The inset in Fig. 6(b) shows the fitting parameter monotonically decreases with time. It is noteworthy that the fitting parameter has actual physical meaning in the volcanic eruption; that is to say,  $V$  is the spherical volume of the lava as a heat point<sup>27</sup>. However, the heat point in the Mogi model cannot be directly measured and examined in our experiments.

**Asymmetrically periodic segregation.** In the APS region, the mixture undergoes a similar time-dependent segregation procedure with that in the SPS region. Fig. 7 shows the order parameter of the APS in five periods for  $P = 50$  kPa and  $\Gamma = 6.2$ . The processes marked I and II represent the percolation and the eruption stage, respectively. The percolation stage of the APS has insignificant difference compared with the SPS. We have investigated the relations between the percolation time and the numbers of two species of particles in atmosphere, where the amount of either alumina or copper particles increases, the percolation time monotonically increases<sup>23</sup>. Nevertheless, the eruption stage of the APS is distinctly different from the SPS. The lower layer of the alumina particles forms a tilting heap at one side of the container, and then the alumina

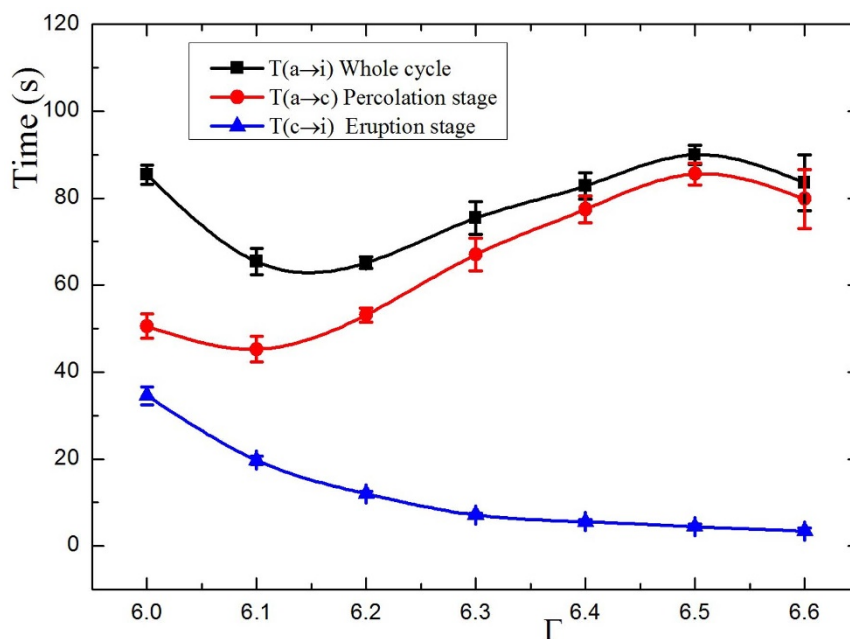


**Figure 5** | Measured periodic time as a function of  $\Gamma$  for SPS pattern. The air pressure  $P$  is 7 kPa and all data points are an average of at least 7 experimental trials. The periodic time of both whole cycle and percolation stage have non-monotonic relations with  $\Gamma$ , whereas the periodic time of the eruption stage monotonically decreases with increasing  $\Gamma$ .

particles surge onto the top surface along either wall of the container, covering the copper layer. Because of the asymmetric profile of the heap, the Mogi model is incapable of fitting the profile evolution of the upper surface during the eruption stage in the APS.

## Discussion

In this experiment, the air effect on the segregation patterns is conclusive. First, all segregation behaviors vanish at sufficiently low

pressure, which is consistent with other observations in the powder system<sup>22–26</sup>. Second, by modulating the air pressure inside the chamber, segregation behaviors can switch between the time-independent segregation pattern (BNE) and the time-dependent segregation pattern (PS). In addition, numerous experimental and theoretical researches have demonstrated that ambient air is of significant importance on the heap formations<sup>28–33</sup>. The air pressure can influence the symmetry of the heap, which distinguishes between the APS

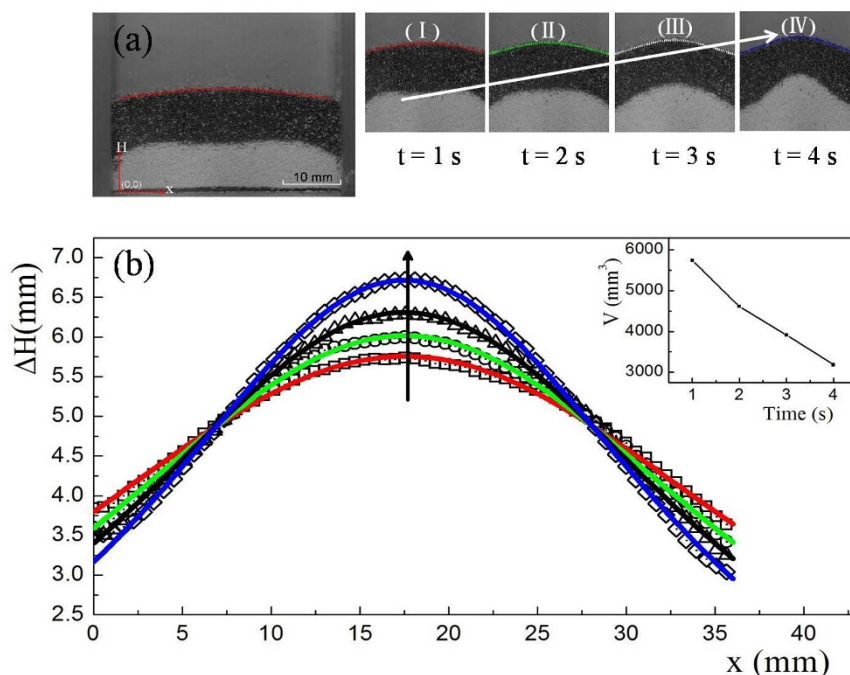


**Figure 6** | Comparison between the topographic profile of the upper surface with the Mogi fitting curves. (a) Illustration of the coordinate system in high speed camera photos. Photos (I) – (IV), a time sequence of pictures clearly shows the upper surface growth with an interval of one second. The solid arcs with different colors are Mogi fitting curves and the arrow is plotted to guide the eye. (b) Comparison of the averaged experimental data (black symbols) and Mogi fitting curves (colourful solid lines). The arrow indicates the evolution of increasing time and the time interval among these four curves is one second. The inset is the fitting parameters  $V$  plotted as a function of time.

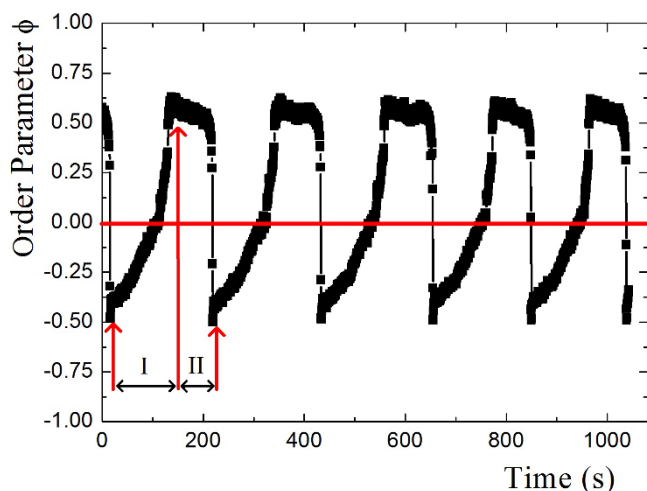


**Figure 7** | Relative height difference  $\phi$ , as an order parameter exhibits an excellent periodicity in the APS pattern at  $P = 50$  kPa and  $\Gamma = 6.2$ . The procedure (I) corresponds to the percolation stage, and (II) corresponds to the eruption stage.

and the SPS pattern in this experiment. Due to the experimental difficulty in measuring the distribution of the air pressure and the air flow inside the granular bed, the quantitative investigation of the air effect on granular segregation has been seldom involved. In our experiment, we preliminarily study a critical value of the air pressure,  $P_c$  as a function of vibration acceleration  $\Gamma$  over which an eruption can occur [see the left boundary of the APS region in Fig. 2].

In summary, we observe a time-dependent periodic segregation behavior, which presents in two different patterns, namely the SPS and the APS, in a vertically vibrated binary granular mixture. A complete cycle of the SPS is described by the successive snapshots. We also plot a  $\Gamma$ - $P$  phase diagram that delineates different segregation behaviors. In the phase diagram, it is clearly shown that the APS and the SPS are reversible by tuning the pressure of interstitial air. Additionally, a well-defined order parameter is introduced to quantitatively describe the time-dependent segregation behaviors, for example, which exhibits the excellent periodicity of both periodic segregation behaviors. With using the order parameter, we also can precisely and conveniently obtain the percolation time and the eruption time in the SPS. With the extracted data, we discuss the relation between the percolation and the eruption time with the vibration acceleration, respectively. Since the eruption stage of the SPS resembles a genuine volcanic eruption in nature, a simplified volcanic model proposed by K. Mogi is used to characterize the profile evolution of the upper surface of the granular volcano, and the experimental evolution of the upper surface agrees well with the expectation of the Mogi model. However, the natural volcanic eruption and the granular eruption, in our experiments, may not share the same physical mechanisms. There could be other theoretical approaches to describe the arching profile of granular eruption by using the continuum theory of surface flows of granular mixtures<sup>8,13</sup>. Finally, we make a comparison between the SPS and the APS pattern, and qualitatively discuss the air effect on the time-dependent segregation behaviors, as well as on the emergence and the symmetry of the heap.

1. Duran, J. *Sands, Powders and Grains* (Springer Verlag, New York, 2000).
2. Jaeger, H. M., Nagel, S. R. & Behringer, R. P. Granular solids, liquids, and gases. *Rev. Mod. Phys.* **68**, 1259 (1996).
3. Kudrolli, A. Size separation in vibrated granular matter. *Rep. Prog. Phys.* **67**, 209 (2004).
4. Börzsönyi, T. & Stannarius, R. Granular materials composed of shape-anisotropic grains. *Soft Matter* **9**, 7401 (2013).

5. Schröter, M., Ulrich, S., Krefit, J., Swift, J. B. & Swinney, H. L. Mechanisms in the size segregation of a binary granular mixture. *Phys. Rev. E* **74**, 011307 (2006).
6. Shi, Q., Sun, G., Hou, M. & Lu, K. Density-driven segregation in vertically vibrated binary granular mixtures. *Phys. Rev. E* **75**, 061302 (2007).
7. Nahmad-Molinari, Y., Canul-Chay, G. & Ruiz-Suárez, J. C. Inertia in the Brazil nut problem. *Phys. Rev. E* **68**, 041301 (2003).
8. Makse, H. A. Continuous Avalanche Segregation of Granular Mixtures in Thin Rotating Drums. *Phys. Rev. Lett.* **83**, 3186 (1999).
9. Seiden, G. & Thomas, P. J. Complexity, segregation, and pattern formation in rotating-drum flows. *Rev. Mod. Phys.* **83**, 1323 (2011).
10. Meier, S. W., Melani-Barreiro, D. A., Ottino, J. M. & Lueptow, R. M. Coarsening of granular segregation patterns in quasi-two-dimensional tumblers. *Nature Phys.* **4**, 244 (2008).
11. Makse, H. A., Havlin, S., King, P. R. & Stanley, H. E. Spontaneous stratification in granular mixtures. *Nature (London)* **386**, 379 (1997).
12. Fan, Y., Boukerkour, Y., Blanc, T., Umbanhowar, P. B., Ottino, J. O. & Lueptow, R. M. Stratification, segregation, and mixing of granular materials in quasi-two-dimensional bounded heaps. *Phys. Rev. E* **86**, 051305 (2012).
13. Boutreux, T., Makse, H. A. & de Gennes, P.-G. Surface flows of granular mixtures: III canonical model. *Eur. Phys. J. B* **9**, 105 (1999).
14. Rosato, A., Strandburg, K. J., Prinz, F. & Swendsen, R. H. Why the Brazil nuts are on top: Size segregation of particulate matter by shaking. *Phys. Rev. Lett.* **58**, 1038 (1987).
15. Trujillo, L., Alam, M. & Herrmann, H. J. Segregation in a fluidized binary granular mixture: Competition between buoyancy and geometric forces. *Europhys. Lett.* **64**, 190 (2003).
16. Knight, J. B., Jaeger, H. M. & Nagel, S. R. Vibration-induced size separation in granular media: The convection connection. *Phys. Rev. Lett.* **70**, 3728 (1993).
17. Caulkin, R., Jia, X., Fairweather, M. & Williams, R. A. Geometric aspects of particle segregation. *Phys. Rev. E* **81**, 051302 (2010).
18. Ulrich, S., Schröter, M. & Swinney, H. L. Influence of friction on granular segregation. *Phys. Rev. E* **76**, 042301 (2007).
19. Yuan, X. X., Zheng, N., Shi, Q. F., Sun, G. & Li, L. S. Segregation in mixtures of granular chains and spherical grains under vertical vibration. *Phys. Rev. E* **87**, 042203 (2013).
20. Huerta, D. A. & Ruiz-Suárez, J. C. Vibration-Induced Granular Segregation: A Phenomenon Driven by Three Mechanisms. *Phys. Rev. Lett.* **92**, 114301 (2004).
21. Hejmady, P., Bandyopadhyay, R., Sabhapandit, S. & Dhar, A. Scaling behavior in the convection-driven Brazil nut effect. *Phys. Rev. E* **86**, 050301(R) (2012).
22. Burtally, N., King, P. J. & Swift, M. R. Spontaneous Air-Driven Separation in Vertically Vibrated Fine Granular Mixtures. *Science* **295**, 1877 (2002).
23. Du, S. S., Shi, Q. F., Sun, G., Li, L. S. & Zheng, N. Percolation current in a periodic segregation of a binary granular mixture. *Phys. Rev. E* **84**, 041307 (2011).
24. Burtally, N., King, P. J., Swift, M. R. & Leaper, M. Dynamical behaviour of fine granular glass/bronze mixtures under vertical vibration. *Granular Matter* **5**, 57 (2003).
25. Biswas, P., Sanchez, P., Swift, M. R. & King, P. J. Numerical simulations of air-driven granular separation. *Phys. Rev. E* **68**, 050301(R) (2003).
26. Klein, M., Tsai, L. L., Rosen, M. S., Pavlin, T., Candela, D. & Walsworth, R. L. Interstitial gas and density segregation of vertically vibrated granular media. *Phys. Rev. E* **74**, 010301(R) (2006).
27. Mogi, K. Relations between the eruption of various volcanoes and the deformation of the ground surface around them. *Bulletin of the Earthquake Research Institute Tokyo* **36**, 34–134 (1958).
28. Aoki, K. M., Akiyama, T., Yama-moto, K. & Yoshikawa, T. Experimental study on the mechanism of convection modes in vibrated granular beds. *Europhys. Lett.* **40**, 159 (1997).
29. Aoki, K. M., Akiyama, T., Maki, Y. & Watanabe, T. Convective roll patterns in vertically vibrated beds of granules. *Phys. Rev. E* **54**, 874 (1996).
30. Pak, H. K., Van Doorn, E. & Behringer, R. P. Effects of Ambient Gases on Granular Materials under Vertical Vibration. *Phys. Rev. Lett.* **74**, 4643 (1995).
31. Zheng, N., Wen, P. P., Shi, Q. F., Lai, P. Y. & Chan, C. K. Heaping instabilities in a layered Bi-disperse granular bed. *EPL* **100**, 44002 (2012).
32. Jia, L.-C., Lai, P. Y. & Chan, C. K. Empty Site Models for Heap Formation in Vertically Vibrating Grains. *Phys. Rev. Lett.* **83**, 3832 (1999).
33. Lai, P. Y., Jia, L. C. & Chan, C. K. Symmetric heaping in grains: A phenomenological model. *Phys. Rev. E* **61**, 5593 (2000).

## Acknowledgments

The work was supported by Chinese National Science Foundation, Project No.11104013.

## Author contributions

P.W. designed and carried out the experiments. P.W., N.Z., L.L. and Q.S. analysed the data and L.L. proposed the model. P.W. and N.Z. contributed to the writing of the manuscript and all authors reviewed the manuscript.

## Additional information

Supplementary information accompanies this paper at <http://www.nature.com/scientificreports>



**Competing financial interests:** The authors declare no competing financial interests.

**How to cite this article:** Wen, P., Zheng, N., Li, L. & Shi, Q. Symmetrically periodic segregation in a vertically vibrated binary granular bed. *Sci. Rep.* 4, 6914; DOI:10.1038/srep06914 (2014).



This work is licensed under a Creative Commons Attribution-NonCommercial-ShareAlike 4.0 International License. The images or other third party material in this article are included in the article's Creative Commons license, unless indicated otherwise in the credit line; if the material is not included under the Creative Commons license, users will need to obtain permission from the license holder in order to reproduce the material. To view a copy of this license, visit <http://creativecommons.org/licenses/by-nc-sa/4.0/>